Earthq Eng & Eng Vib (2021) 20: 403-421 **DOI**: https://doi.org/10.1007/s11803-021-2028-5

Normalized residual displacement spectra for post-mainshock assessment of structures subjected to aftershocks

Saeed Amiri[1†], Alireza Garakaninezhad[2‡] and Edén Bojórquez[3§]

1. *Structural Engineering Research Center, International Institute of Earthquake Engineering and Seismology (IIEES), Tehran, Iran*
2. *Department of Civil Engineering, Faculty of Engineering, University of Jiroft, Jiroft, Kerman, Iran*
3. *Facultad de Ingeniería, Universidad Autónoma de Sinaloa, Calz. de las Américas y Boulevard Universitarios, Cd. Universitaria, 80040 Culiacán, Mexico*

Abstract: Residual displacement, as a significant measure of structural inelasticity, is effectively used in post-earthquake seismic assessment of structures. This demand can be considered for seismic evaluation of structures under multiple earthquakes. This study introduces a simple and novel index to predict the residual displacement of mainshock-damaged structures against subsequent aftershock. The proposed index is defined as a ratio between residual displacement of damaged structures against aftershock and peak inelastic displacement of intact structures under mainshock. In this study, constant-strength spectra based on the index are developed considering the effects of important structural characteristics and also significant seismic parameters. Moreover, analytical equations are presented to predict the proposed index for bi-linear single-degree-of-freedom (SDOF) systems considering both the effects of positive and negative polarities of aftershock. Furthermore, an equation is suggested to estimate the peak inelastic displacement of intact systems under mainshock, which is required to compute the index.

Keywords: residual displacement demand; mainshock-aftershock sequences; peak inelastic displacement; constant-strength spectra

1 Introduction

Residual displacement is a key measure of structural damage, which plays a pivotal role in seismic assessment of structures. This demand can be effectively used in post-earthquake decision making to repair or demolish damaged structures, as stated in FEMA P-58 (FEMA, 2012). Several studies have focused on investigating the residual displacement / drift of reinforced concrete (RC) frames (Dai *et al*., 2017; Tesfamariam and Goda, 2015; Ramirez and Miranda, 2012), steel frames (Bravo-Haro and Elghazouli, 2018; Ruiz-García and Chora, 2015; Bojórquez and Ruiz-García, 2013; López-Barraza *et al*., 2013; Erochko *et al*., 2011), and bridge structures (Ardakani *et al*., 2021; Cai *et al*., 2019; Shu and Zhang, 2018; Cheng *et al*., 2016; Lee and Billington, 2011). In addition, numerous researchers have investigated the residual displacement of SDOF systems (Harikrishnan and Gupta, 2020; Amiri and Bojórquez, 2019; Guo and Christopoulos, 2018; Ji *et al*., 2018; Guerrero *et al*., 2017; Ruiz-García and Guerrero, 2017; Huff, 2016; Liossatou and Fardis, 2016; Liossatou and Fardis, 2015; Ruiz-García and Miranda, 2006; Christopoulos *et al*., 2003). Ruiz-García and Miranda (2006) evaluated the residual displacement ratio (C_r) of SDOF oscillators considering the variability of structural and important seismic parameters. They proposed an equation to estimate C_r. Liossatou and Fardis (2015 and 2016) recently carried out an extensive parametric study on the residual displacement of SDOF systems considering various hysteretic models of typical RC structures. This research showed that the presence of a velocity pulse in earthquake motions increases the peak inelastic displacement as well as the residual displacement by similar proportion. In addition, C_r is dependent on the pulse period.

Recently, Ruiz-García and Guerrero (2017) examined the spectral trend of C_r for elastoplastic SDOF systems against earthquakes recorded on soft soil. They proposed an analytical equation to predict the residual displacement ratios of these structures in Mexico City and the San Francisco Bay Area. In another study, a probabilistic framework was introduced by Guo and Christopoulos (2018) to estimate the ratio of residual displacement to peak displacement of bi-linear and tri-linear SDOF systems as non-degrading structures with and without

Correspondence to: Edén Bojórquez, Facultad de Ingeniería, Universidad Autónoma de Sinaloa, Calz. de las Américas y Boulevard Universitarios, Cd. Universitaria, 80040 Culiacán, Mexico
Tel: +52-1-6672080401
E-mail: eden@uas.edu.mx
[†]M.Sc. Graduate; [‡]Assistant Professor; [§]Professor
Received November 3, 2019; **Accepted** June 23, 2020

supplemental dampers using post-peak oscillation analysis. A probability model was proposed to capture statistical trends of the normalized residual displacement under near-fault pulse like and far-field ground motions considering different structural parameters. Moreover, Ji *et al*. (2018) assessed the residual displacement ratios of nonlinear SDOF oscillators built on soft soil sites. A statistical equation was presented to predict C_r for different post-yield stiffness ratios and hysteretic laws. In a recent study, Amiri and Bojórquez (2019) investigated the residual displacement ratios of bi-linear SDOF systems against mainshock-aftershock sequences using constant-strength spectra. They proposed some analytical equations to estimate C_r under seismic sequences considering the variations of elastic vibration period, strength reduction factor, post-yield stiffness ratio, and aftershock intensity.

A mainshock can trigger aftershocks during a short time span which may cause additional damage to mainshock-damaged structures. The historical seismic sequences show the secondary structural damage. In 1985, the Michoacán mainshock in Mexico City with a moment magnitude (M_w) of 8.0 was followed by an aftershock with M_w 7.6. Numerous medium-rise RC buildings suffered structural damage during this mainshock (Rosenblueth and Meli, 1986). The aftershock caused the collapse of many of these RC buildings (Ruiz-García *et al*., 2012). An example of recent major mainshock-aftershock sequences occurred in New Zealand in 2010. The M_w 7.1 Darfield event triggered two aftershocks with M_w 6.2 and 6.0 and damaged many structures (Atzori *et al*., 2012). Another disaster was reported in 2011 in Japan due to the Tohoku great earthquake with M_w 9.0 and its aftershocks (Goda *et al*., 2013). Recently, the 2016 Central Italy earthquake sequence consisted of a series of moderate-to-large seismic motions, between M_w 5.0 and M_w 6.5, led to damage to historical centers and roadway infrastructure (De Risi *et al*., 2018; Durante *et al*., 2018; Mazzoni *et al*., 2018). These observations indicate that the reliable seismic assessment of structures must be conducted by considering the effects of aftershocks. Another weak point in this regard is that the current seismic regulations do not consider multiple earthquakes (Amiri and Soroushian, 2017; Oyarzo-Vera and Chouw, 2008; Doğangün and Livaoğlu, 2006).

Many researchers have focused on seismic evaluation of structures against successive earthquakes in the context of SDOF systems (Di Sarno *et al*., 2020; Di Sarno and Amiri, 2019; Amiri and Bojórquez, 2019; Durucan and Gümüş, 2018; Yu *et al*., 2018; Zhai *et al*., 2015; Di Sarno, 2013; Goda and Taylor, 2012), RC, steel and wood frames (Shokrabadi and Burton, 2018; Ruiz-García *et al*., 2018; Tesfamariam and Goda, 2017; Nazari *et al*., 2015; Raghunandan *et al*., 2015; Goda and Salami, 2014; Li *et al*., 2014; Salami and Goda, 2013; Ruiz-García and Negrete-Manriquez, 2011), infilled buildings (Di Trapani and Malavisi, 2019; Furtado *et al*., 2018; Burton and Sharma, 2017; Furtado *et al*., 2017; Tesfamariam *et al*., 2015), concrete gravity dams (Wang *et al*., 2018; Wang *et al*., 2017; Zhang *et al*., 2013), healthcare facilities (Santarsiero *et al*., 2018), bridges (Omranian *et al*., 2018; Tolentino *et al*., 2018; Ghosh *et al*., 2015; Alessandri *et al*., 2013; Franchin and Pinto, 2009), tunnels (Singh *et al*., 2018), and ancient multi-drum columns (Papaloizou *et al*., 2016). Several studies (Wen *et al*., 2020; Zhai *et al*., 2018; Wen *et al*., 2018; Wen *et al*., 2017) have been conducted on the seismic investigation of structures against multiple earthquakes accounting for the cumulative-based response, such as the modified Park-Ang damage index (Kunnath *et al*., 1992); however, limited works (Amiri and Bojórquez, 2019; Pu and Wu, 2018) focused on developing response spectra based on the residual displacement for sequential earthquakes. Considering the role of this seismic demand on structural damage, as well as its being practical, it is necessary to conduct more studies regarding the residual displacement of structures under repeated ground motions. Moreover, another significant issue regarding multiple earthquakes is the aftershock polarity with respect to the mainshock. The aftershock can be applied in the same direction of the mainshock, referred to as positive polarity, or in the opposite direction of the mainshock, referred to as negative polarity. This phenomenon becomes more important if the residual displacement/drift is considered as a structural seismic demand (Raghunandan *et al*., 2012; Ruiz-García and Aguilar, 2015; Wen *et al*., 2018).

The time period between the mainshock and subsequent aftershock is usually short, and subsequently the decision-making process on structures damaged due to a first seismic event is a crucial task. In addition, this short time interval between two consecutive events may not allow engineers time for in-situ measurement of most damaged structures within regions affected by an earthquake. Therefore, the availability of simple and robust methods is necessary for rapid assessment of mainshock-damaged structures. The objective of the present study is to propose a simple and novel index to estimate the residual displacement of damaged structures against subsequent aftershock considering the peak inelastic displacement of intact structures under mainshock. The index can be used for post-mainshock assessment of structures as SDOF systems, and recovery process and building tagging. In other words, engineers can predict the residual displacement of structures, damaged due to mainshock, against following aftershocks. Furthermore, the effect of aftershock polarity is taken into account in analytical equations presented to predict the index.

2 Proposed index

The index is the ratio between the residual displacement of mainshock-damaged structures subjected to aftershocks and the peak inelastic

displacement of intact structures against the mainshock, which is expressed as follows:

$$I_{ra} = \frac{\delta_{res,a}}{\delta_{max,m}} \quad (1)$$

where I_{ra} is the proposed index, $\delta_{res,a}$ stands for the residual displacement of the structure subjected to the aftershock, and $\delta_{max,m}$ denotes the peak inelastic displacement of intact structures under the mainshock. The direct prediction of the residual displacement of the structure against the aftershock is carried out by multiplying $\delta_{max,m}$ by I_{ra}. $\delta_{max,m}$ is also estimated by the equations presented in this study. In the current study, constant-strength spectra in terms of I_{ra} are developed considering a wide range of structural parameters, as shown in Table 1. The SDOF systems with an elastoplastic model are considered herein and the viscous damping ratio (ξ) in all cases is constant and is equal to 5%. The structural systems are modeled by the OpenSees (Open System for Earthquake Engineering Simulation) software (Mazzoni *et al.*, 2006). In addition, inelasticity behavior is assigned using the Steel01 material model which is available in this software. Figure 1 delineates an example to show $\delta_{max,m}$ and $\delta_{res,a}$. In this figure, the displacement history of a SDOF system with T=1.5 s and R=3.0 under a seismic sequence is depicted, and $\delta_{max,m}$ and $\delta_{res,a}$ are also indicated. The flowchart of computing the proposed index is presented in Fig. 2. In this figure, m is the mass of the system, S_a denotes the spectral acceleration, and F_y implies the lateral yield strength.

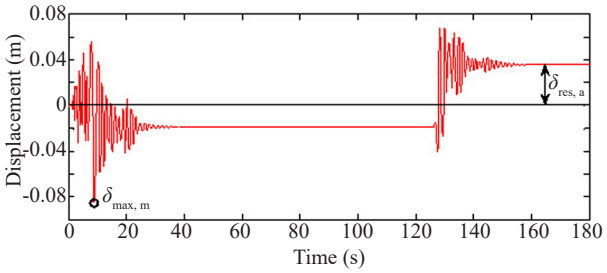

Fig. 1 Example to show $\delta_{max,m}$ and $\delta_{res,a}$

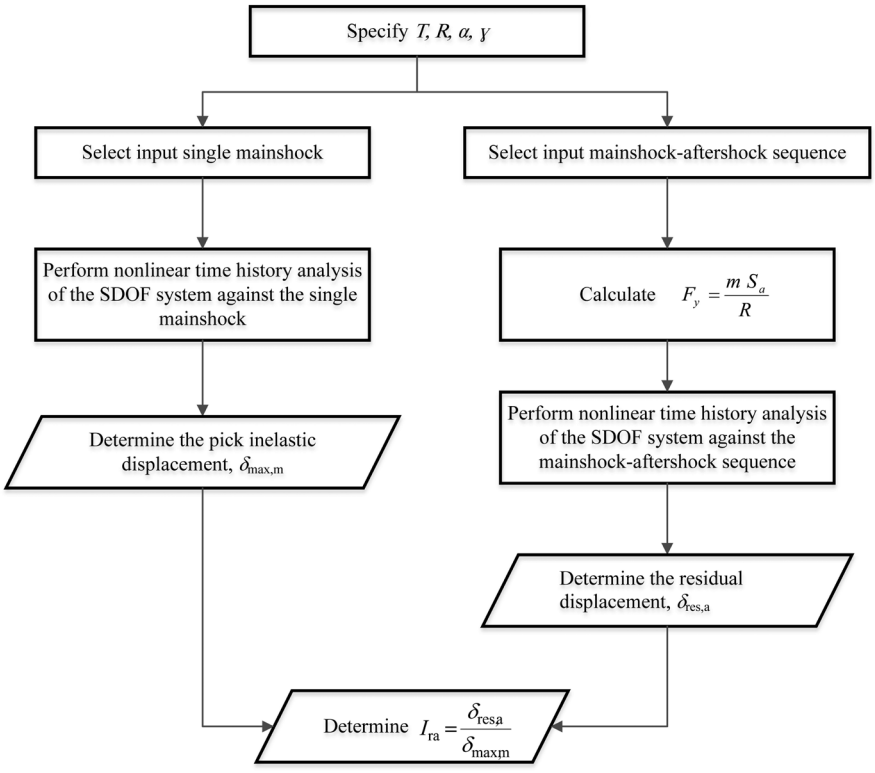

Fig. 2 Flowchart of computing the proposed index

Table 1 Structural parameters of SDOF systems

Structural parameter	Range of parameter
Natural vibration period (T)	0.1–3.0 s with a period step of 0.1 s
Strength reduction factor (R)	2,3,4,5,6
Post yield stiffness ratio (α)	0, 0.03, 0.05

3 Seismic sequences

In this study, as-recorded seismic sequences are used to investigate the proposed index. As noted in previous studies (Goda and Taylor, 2012; Jalayer and Ebrahimian, 2017; Li and Ellingwood, 2007; Ruiz-García *et al*., 2014; Ruiz-García and Negrete-Manriquez, 2011), unreliable responses can be obtained using artificial seismic sequences. Therefore, a large set of 330 real mainshock-aftershock records is selected from the Pacific Earthquake Engineering Research (PEER) (PEER Ground Motion Database (https://ngawest2.berkeley.edu/)) according to following criteria (Goda and Taylor, 2012): (1) average horizontal peak ground acceleration (PGA) and average horizontal peak ground velocity (PGV) are greater than or equal to 0.04 g and 1.0 cm/s, respectively; (2) moment magnitude (M_w) is greater than or equal to 5.0; (3) ground motions were recorded on site classes C and D according to ASCE/SEI 7-10 (ASCE/SEI 7-10, 2010), and (4) closest site-to-fault-rupture distance is less than 75 km. Table 2 describes the seismic sequences used in this study. The total number of records in the last column of this table is 165 two-component seismic motions (horizontal components). Hence, a total of 330 records are used for nonlinear time history analyses. Moreover, a 60 second time gap with zero acceleration is considered between the mainshock and the aftershock motions to allow the systems to cease moving after the first event. In addition, an interval of 20 seconds is inserted after the end of the aftershocks to capture the residual displacement demands. Note that in order to consider the effect of aftershock negative polarity, the opposite directions of aftershocks are artificially considered as well. More information about multiple earthquakes is found in Goda and Taylor (2012). The moment magnitude–distance distribution and the moment magnitude–PGA distribution of the mainshocks and aftershocks are shown in Fig. 3. For each seismic record, one sequence (including one mainshock and one aftershock) is considered. Furthermore, to vary the aftershock PGA (PGA_a) with respect to the mainshock PGA (PGA_m), which is shown by Eq. (2), five values of this ratio (γ) are considered herein: γ=0.5, 0.8, 1.0, 1.2, and 1.5.

$$\gamma=\frac{PGA_a}{PGA_m} \tag{2}$$

4 Effects of ground motion and structural parameters on I_{ra}

The wide sensitivity analyses are carried out in this study to examine the effects of important earthquake parameters as well as significant structural characteristics on the proposed index (I_{ra}). The ground motion parameters include the moment magnitude (M_w), site condition, epicentral distance, duration, and aftershock relative PGA (γ). The structural characteristics are the strength reduction factor (R) and post-yield stiffness ratio (α). Note that extensive parametric studies are conduced herein, but for the sake of succinctness, all results are not presented in the study, and the investigations are limited

Table 2 Real seismic sequences used in this study

Earthquake	Time	Number of selected ground motions		
		Site C	Site D	Total
Imperial Valley	1979.10.15	0	12	12
Coalinga	1983.05.02	0	1	1
Coalinga	1983.05.09	5	2	7
Coalinga	1983.07.09	4	0	4
Superstition Hills	1987.11.24	0	1	1
Chalfant Valley	1986.07.20	0	5	5
Irpinia	1980.11.23	2	1	3
Friuli	1976.09.11	2	1	3
Managua	1972.12.23	0	1	1
Whittier Narrows	1987.10.01	3	6	9
Livermore	1980.01.24	0	2	2
Kozani	1995.05.13	0	1	1
Northridge	1994.01.17	4	8	12
Kocaeli & Duzce	1999.08.17	0	1	1
Chi-Chi	1999.09.20	46	54	100
Mammoth Lakes	1980.05.25	0	2	2
Mammoth Lakes	1983.01.07	0	1	1

to R=3.0, 5.0, and γ=0.5 in Subsections 4.1 to 4.4. Also, the comparisons are reported for only the positive polarity in Section 4. However, as an example in Subsection 4.1, it is shown that the difference between the index values for positive and negative polarities in case of one of the magnitude-based subsets, i.e., moderate mainshock and moderate aftershock, can be different.

4.1 Effect of moment magnitude

The moment magnitude of the mainshock (M_w^m) and aftershock (M_w^a) are classified into three subsets to investigate M_w on I_{ra}. The subsets are: (a) moderate mainshock and moderate aftershock ($M_w^m < 6.3$ and $M_w^a < 6.3$), denoted by moderate-moderate, including 76 records, (b) severe mainshock and moderate aftershock ($M_w^m \geq 6.3$ and $M_w^a < 6.3$), denoted by severe-moderate, including 238 records, and (c) severe mainshock and severe subsequent aftershock ($M_w^m \geq 6.3$ and $M_w^a \geq 6.3$), denoted by severe-severe, including 16 ground motions. The severe-severe subset is eliminated from comparison, because only a few records belong to this subset. As expected, the number of sequences of the severe-moderate subset is more than records existing in the other subsets.

The mean inelastic spectra in terms of the normalized residual displacement (I_{ra}) for these classifications are indicated in Figs. 4 and 5. The figures show that the effect of ground motion magnitude, denoted by M_w^m and M_w^a, on I_{ra} for the moderate-to-long period structures with linear elastic-perfectly plastic behavior (T>1.0 s, α=0) is of great importance. For these structural systems, the seismic sequences characterized by the Moderate-Moderate subset lead to higher values of I_{ra} with about 43% and 37% in comparison with another subset (severe-moderate) for R=3.0 and R=5.0, respectively. Considering the aftershock moment magnitudes of two subsets are the same; hence, the difference of their responses arises from the mainshock moment magnitude. The values of peak inelastic displacement obtained from the moderate mainshock (which exists in the Moderate-Moderate subset) are lower than those of the Severe-Moderate sequences. Thus, for the Moderate-Moderate case, the denominator of the index (I_{ra}) is lower, and I_{ra} values are generally larger in this subset, especially for long-period SDOF systems, as shown in the figures. Moreover, Fig. 6 reveals that the index values for positive and negative polarities in the case of one of the magnitude-based subsets, i.e., moderate mainshock and moderate aftershock, can be different.

4.2 Effect of site condition

As mentioned in Section 3, the mainshock-aftershock sequences used in the study were recorded on site classes C and D, considering the average velocity of shear waves in the top 30 m of soil (V_{S30}), as proposed in ASCE/SEI 7-10 (2010). Two subsets are formed in this regard to investigate the effect of site conditions on I_{ra}: (a) ground motions recorded on site class C (132 records), and (b) ground motions recorded on site class D (198 records). Figures 7 and 8 show the mean inelastic spectra based on the normalized residual displacement, i.e., I_{ra} for the site class-based subsets. It is observed that for the long-period structures (T>1.5 s) as well as smaller values of strength reduction factors (R=3), which were built on site class C, there are more values of I_{ra} (13% on average for three values of α) in comparison with their equivalents built in site class D (see Fig. 7).

4.3 Effect of epicentral distance

To investigate the effect of epicentral distances of the mainshocks, shown by (R_m), and subsequent aftershocks, shown by (R_a), four subsets are categorized: (a) near-field mainshock and near-field aftershock (R_m<20 km and R_a<20 km), abbreviated by near-near, including 90 ground motions, (b) far-field mainshock and near-field aftershock (R_m≥20 km and R_a<20 km), abbreviated by far-near, including eight ground motions, (c) near-field mainshock and far-field aftershock (R_m<20 km and

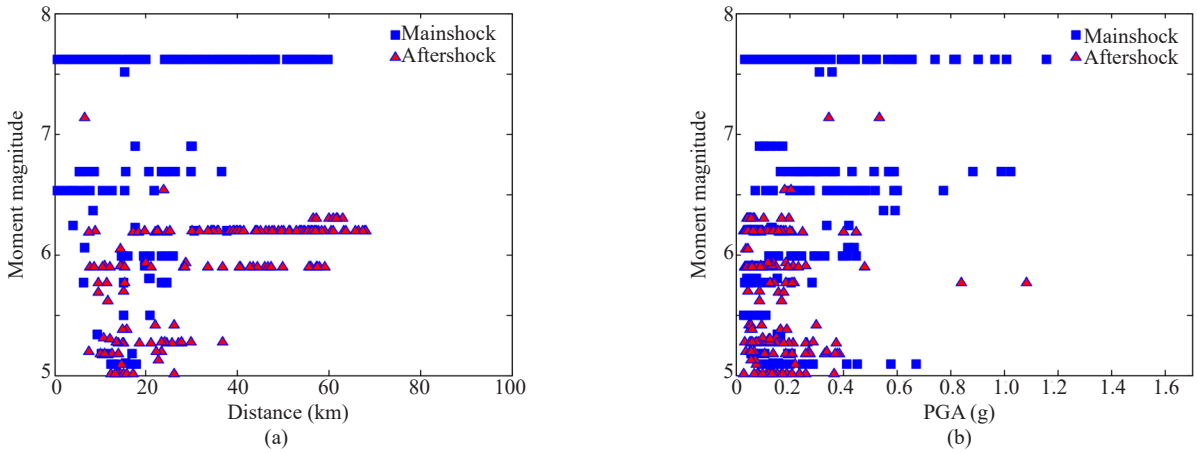

Fig. 3 Comparison between the parameters of mainshock and aftershock motions: (a) moment magnitude–distance distribution; (b) moment magnitude–PGA distribution

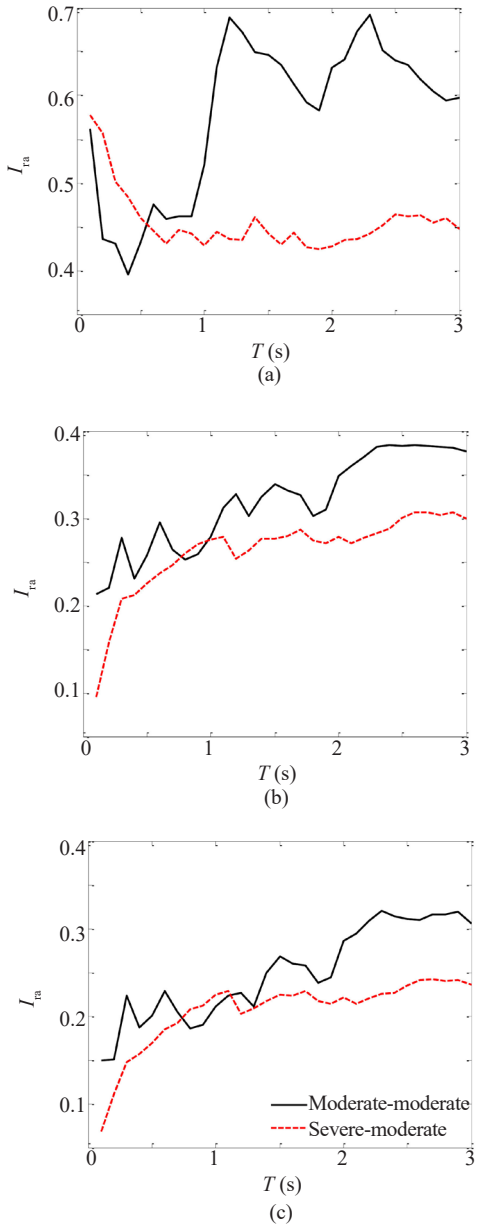

Fig. 4 Mean inelastic spectra in terms of I_{ra} for the magnitude-based subsets, in the case of γ=0.5 and R=3.0: (a) α=0; (b) α=0.03; (c) α=0.05

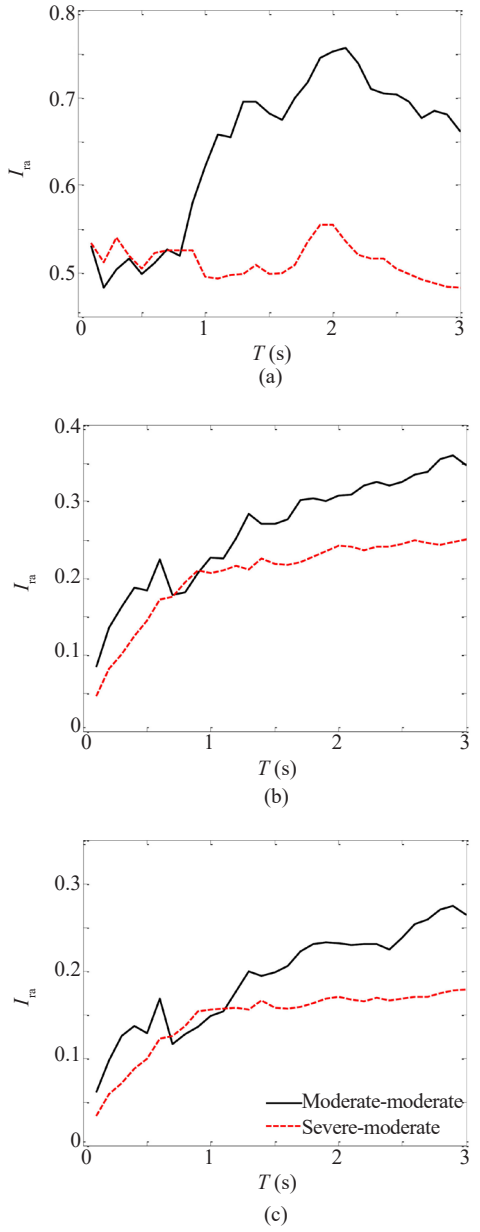

Fig. 5 Mean inelastic spectra in terms of I_{ra} for the magnitude-based subsets, in the case of γ=0.5 and R=5.0: (a) α=0; (b) α=0.03; (c) α=0.05

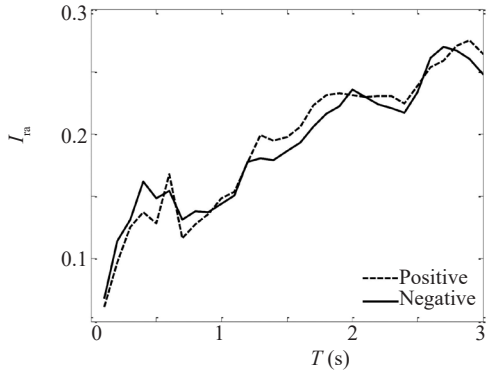

Fig. 6 Mean inelastic spectra in terms of I_{ra} for positive and negative polarities, in the case of γ=0.5, R=5.0 and α=0.05

$R_a \geq 20$ km), abbreviated by near-far, including 82 ground motions, (d) far-field mainshock and far-field aftershock ($R_m \geq 20$ km and $R_a \geq 20$ km), denoted by far-far, including 150 ground motions. The far-near subset is excluded from the investigation, because only a few records are included in this subset.

Figures 9 and 10 show the mean inelastic spectra in terms of I_{ra} for three epicentral distance subsets. According to these figures, the SDOF systems with the linear elastic-perfectly plastic behavior (α=0) in the range of $T \geq 1.0$ s under near-near seismic sequences are more vulnerable during post-mainshock conditions. On average, the I_{ra} values predicted for these structural

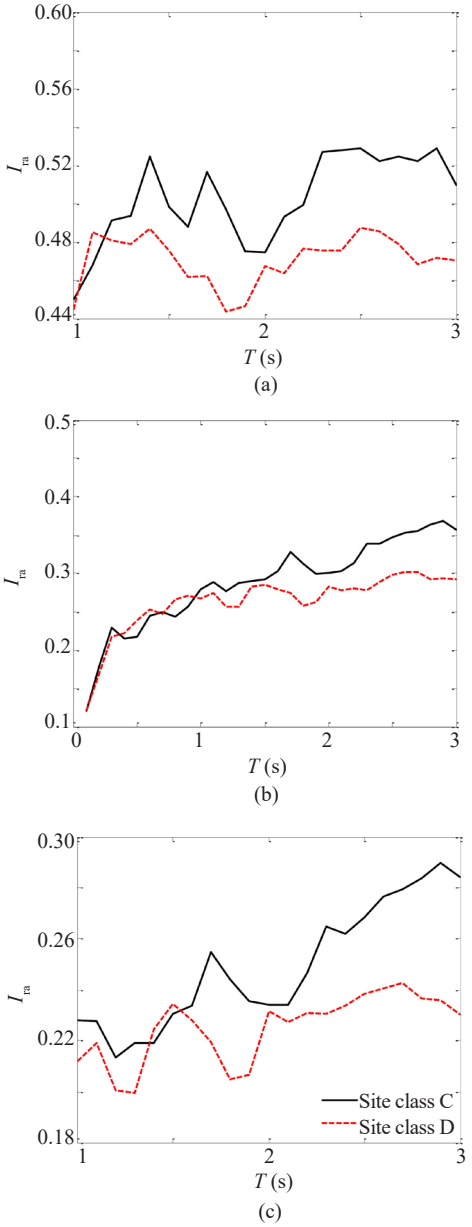

Fig. 7 Mean inelastic spectra in terms of I_{ra} for the site class-based subsets, in the case of γ=0.5 and R=3.0: (a) α=0; (b) α=0.03; (c) α=0.05

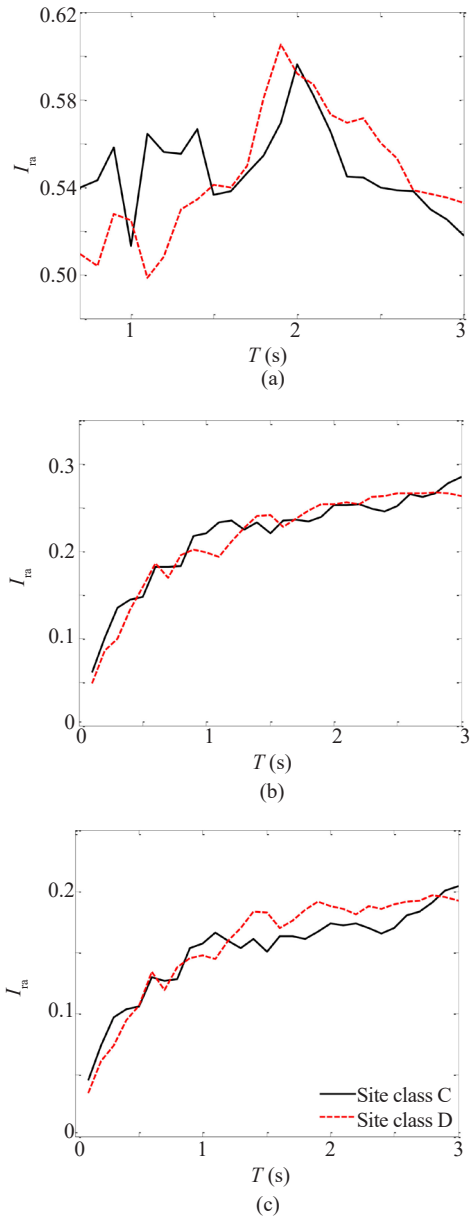

Fig. 8 Mean inelastic spectra in terms of I_{ra} for the site class-based subsets, in the case of γ=0.5 and R=5.0: (a) α=0; (b) α=0.03; (c) α=0.05

systems under the near-near subset are 28% and 48% larger than the near-far and far-far subsets, respectively (see Figs. 9(a) and 10(a)). The most probable reason for this phenomenon is due to near-field effects and higher PGA when compared to the other subsets. This percentage decreases as the post-yield stiffness ratio increases, as depicted in Figs. 9(b), 9(c), 10(b), and 10(c).

4.4 Effect of duration

The earthquake duration has been defined in several ways (Bommer and MartÍNez-Pereira, 1999). One of the most common of the definitions is the significant duration (*D*5-95) (Trifunac and Brady, 1975), which is employed in this work. This parameter is considered as a time interval between 5% and 95% of the Arias intensity (*IA*). *IA* is stated as:

$$IA = \frac{\pi}{2g}\int_0^{t_{max}} a^2(t)\mathrm{d}t \tag{3}$$

where t_{max} is the length of the accelerogram, g is the acceleration due to gravity, and $a(t)$ implies the ground acceleration time history.

The seismic sequences are divided into four subsets regarding the significant duration of the mainshock (*D*5-95_m) and subsequent aftershock (*D*5-95_a) to assess the

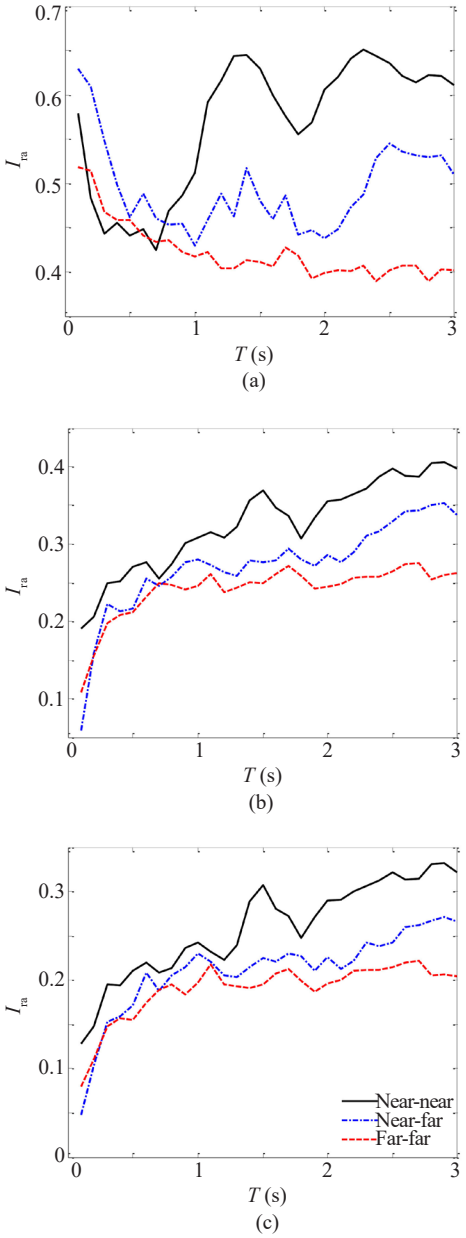

Fig. 9 Mean inelastic spectra in terms of I_{ra} for the epicentral distance-based subsets, in the case of γ=0.5 and R=3.0: (a) α=0; (b) α=0.03; (c) α=0.05

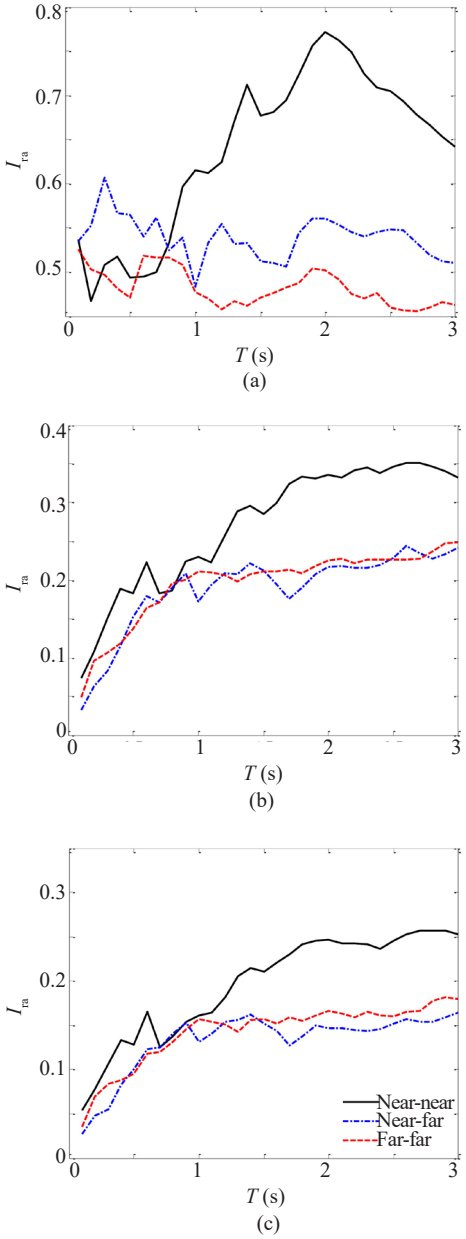

Fig. 10 Mean inelastic spectra in terms of I_{ra} for the epicentral distance-based subsets, in the case of γ=0.5 and R=5.0: (a) α=0; (b) α=0.03; (c) α=0.05

influence of earthquake significant duration on I_{ra}. The subsets are: (a) short duration mainshock and short duration aftershock ($D5\text{-}95_m \leq 25$ s and $D5\text{-}95_a \leq 25$ s), abbreviated by SD-SD, including 175 records, (b) short duration mainshock and long duration aftershock ($D5\text{-}95_m \leq 25$ s and $D5\text{-}95_a > 25$ s), abbreviated by SD-LD, including six records, (c) long duration mainshock and short duration aftershock ($D5\text{-}95_m > 25$ s and $D5\text{-}95_a \leq 25$ s), abbreviated by LD-SD, including 94 records, and (d) long duration mainshock and long duration aftershock ($D5\text{-}95_m > 25$ s and $D5\text{-}95_a > 25$ s), abbreviated by LD-LD, including 55 records. The SD-LD subset is not considered for investigation, due to its small number of records.

The effect of the mainshock-aftershock significant duration on the normalized residual displacement (I_{ra}) is shown in Figs. 11 and 12. The figures indicate that the short duration mainshocks and short duration aftershocks lead to larger I_{ra} for moderate-to-long period structures ($T \geq 1.0$ s) when compared to other duration-based subsets. In this regard, the responses obtained from the SD-SD subset are wider by on average 28% and 65% than the LD-SD and LD-LD subsets, respectively. This proves that the seismic vulnerability of the long period structures after short duration mainshocks will be noticeably affected during subsequent short duration aftershocks.

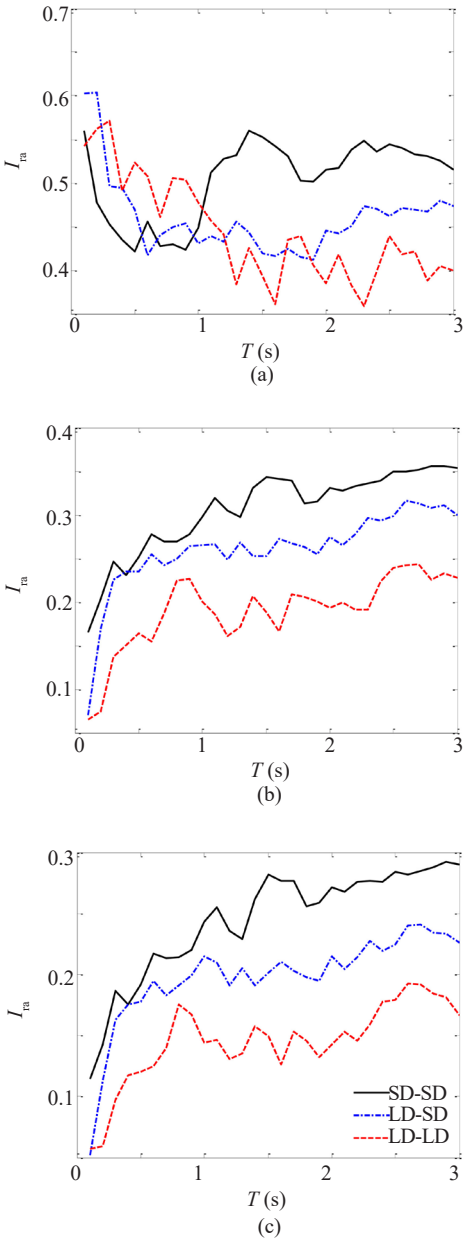

Fig. 11 Mean inelastic spectra in terms of I_{ra} for the duration-based subsets, in the case of γ=0.5 and R=3.0: (a) α=0; (b) α=0.03; (c) α=0.05

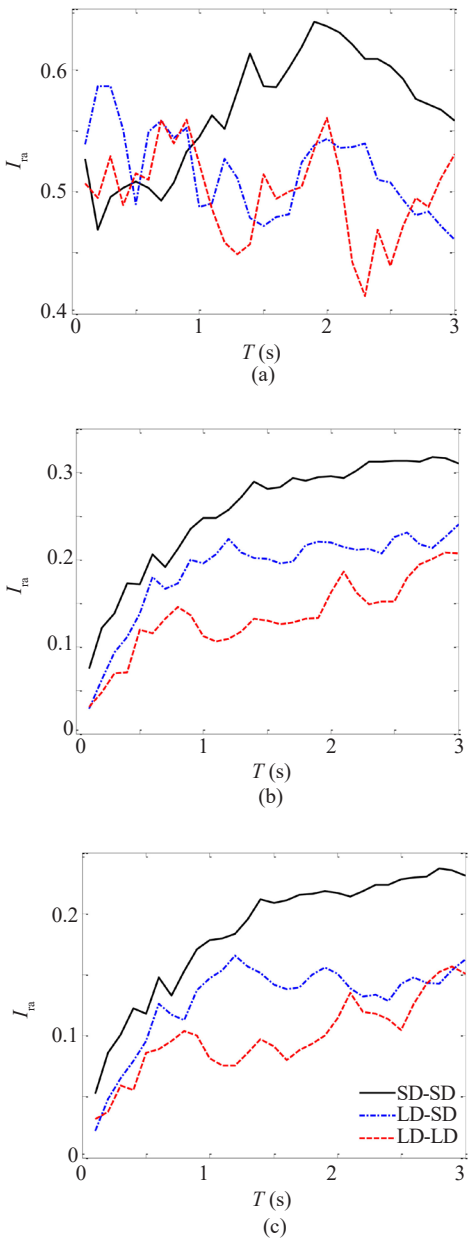

Fig. 12 Mean inelastic spectra in terms of I_{ra} for the duration-based subsets, in the case of γ=0.5 and R=5.0: (a) α=0; (b) α=0.03; (c) α=0.05

4.5 Effect of aftershock relative PGA

Five values of aftershock relative PGA (γ=0.5, 0.8, 1.0, 1.2, 1.5) are considered in this study to evaluate the effect of aftershock intensity in terms of PGA_a/PGA_m on I_{ra}. This variation provides a reliable range of I_{ra} for decision makers. The investigation is carried out only for R=3.0, due to succinctness, as shown in Fig. 13. It can be observed from the figure that when α=0, the effect of γ is significant, such that the normalized residual displacement (I_{ra}) increases as the aftershock relative PGA increases. As a comparison, for the systems with the linear elastic-perfectly plastic model, the values of I_{ra} obtained from γ=1.5 are greater (57% on average) than γ=0.5. This influence is minor in the case of α>0 (i.e., α=0.03, 0.05 herein). In general, the greater aftershock relative PGA would cause more structural damage in terms of residual displacement.

4.6 Effect of post-yield stiffness ratio

The sensitivity of I_{ra} on the post-yield stiffness ratio (α) is presented in Fig. 14, when γ=0.5. In view of this figure, higher I_{ra} values are expected with decreasing α. This is highlighted for weaker systems (R=6.0), such that these structures with the linear elastic-perfectly

plastic model (α=0) experience larger I_{ra} than α=0.03 and α=0.05, by 232% and 369%, respectively. This shows that the increase of the post-yield stiffness ratio using several high-strength elastic materials can be an efficient way to decrease the residual displacement demand of structures and can thus be a choice for designing resilient structures (Qiang *et al*., 2019).

4.7 Effect of strength reduction factor

Figure 15 indicates the mean inelastic spectra based on I_{ra} for different values of R (R=2, 3, 4, 5, 6). It can be observed that the normalized residual displacement increases as R tends to increase in the case of α=0, especially for lower R (from R=2.0 to R=3.0, the increase percent is about 25% for all T values). This trend is inverse for α=0.03, and α=0.05, namely, I_{ra} decreases as R increases (from R=2.0 to R=6.0, the decrease percentage are approximately 66% and 98% for α=0.03 and α=0.05, respectively, in total interval of T). In addition, it is expected that I_{ra} increases for flexible systems (increasing T) with α>0.0 (α=0.03 and α=0.05). Furthermore, it is found that the structures with larger R as well as α=0 possess the worst conditions from point of view of safety during seismic sequences.

5 Prediction equations

The availability of closed-form equations for rapid seismic assessment of structures damaged under

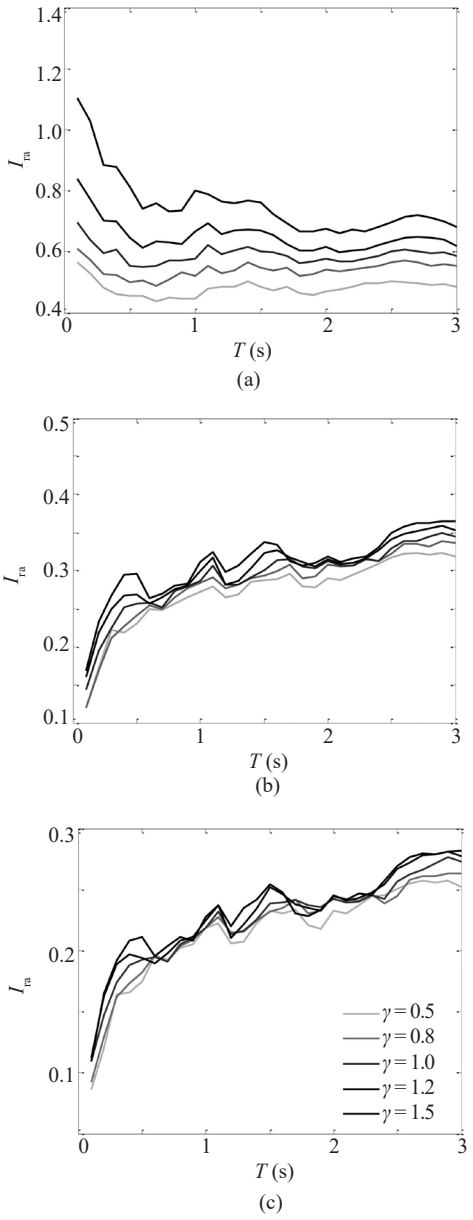

Fig. 13 Effect of the aftershock relative PGA on I_{ra}, when R=3.0, (a) α=0; (b) α=0.03; (c) α=0.05

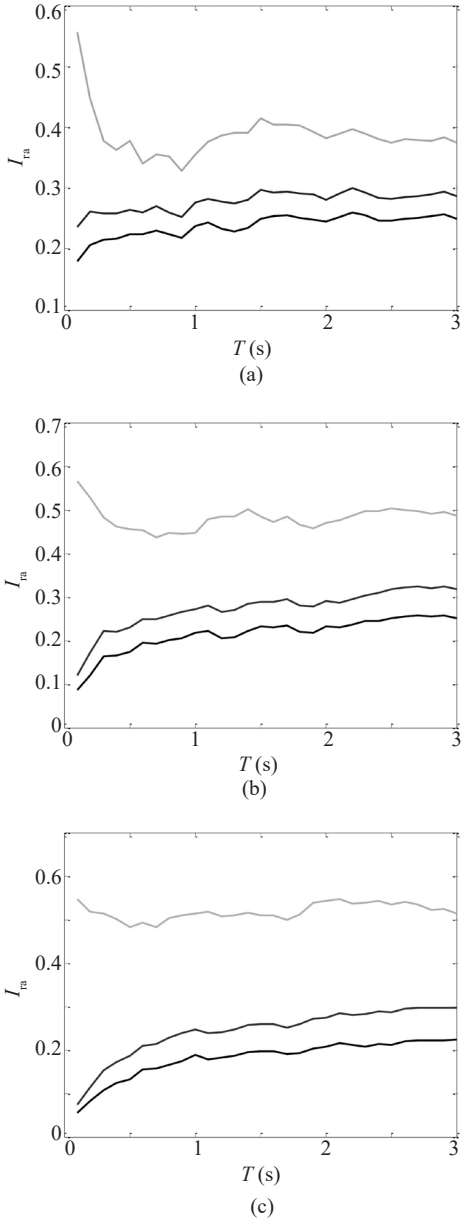

Fig. 14 Effect of post-yield stiffness ratio on I_{ra}, when γ=0.5: (a) R=2.0; (b) R=3.0; (c) R=4.0; (d) R=5.0 and (e) R=6.0

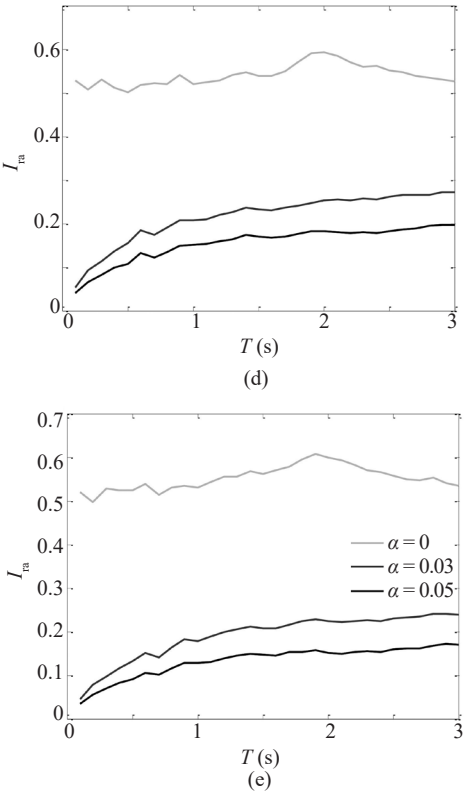

Fig. 14 Continued

a mainshock is essential, due to the short time period between the mainshock and the aftershock. The current study introduces several equations to predict the proposed index (I_{ra}) for both cases of positive and negative polarities of aftershock, and also the inelastic maximum displacement of intact structures (as SDOF systems) against the mainshock, which is required to compute the index. Thus, based on the research results, extensive nonlinear regression analyses are carried out using the method of Least-Squares Fitting to find efficient models. Another criterion for selecting the configuration of Eq. (4) is that the residual displacement, and consequently the proposed index, would be zero in the elastic range (R=1). Therefore, the equation should satisfy this boundary condition.

Note that the equations can be extended for a class of steel or RC buildings to estimate probable residual displacement/drift demands of these structures against aftershock, and subsequently for the recovery process and building tagging. The mean values of I_{ra} are predicted by Eq. (4) for the positive and negative polarities of aftershock. This equation is a function of T and R, so that the unknown coefficients values (a_1, a_2, …, a_7) and (b_1, b_2, …, b_7) for different aftershock relative PGAs (γ), and also post-yield stiffness ratios (α) are obtained from Tables 3 and 4 for the positive and negative polarities, respectively. Note that considering various γ values as well as both positive and negative polarities of aftershocks provide an appropriate range of I_{ra} to make a better decision on mainshock-damaged

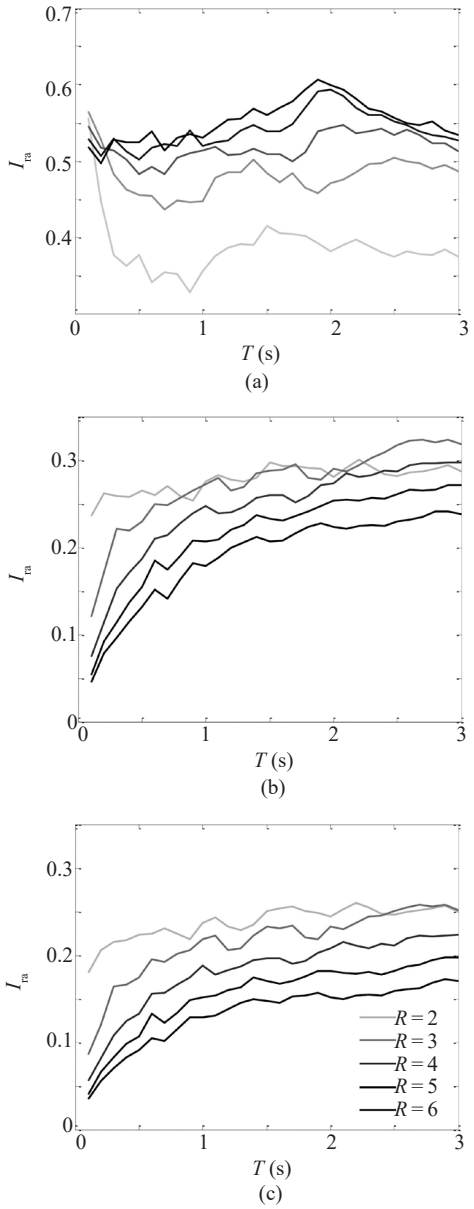

Fig. 15 Mean inelastic spectra in terms of I_{ra} for different strength reduction factors, when γ=0.5: (a) α=0; (b) α=0.03; (c) α=0.05

structures and seismic risk assessment of these structures against subsequent aftershocks. The inelastic maximum displacement of SDOF systems under mainshock ($\delta_{max,m}$) is required to compute I_{ra} (see Eq. (1)), which can be calculated by Eq. (5). Table 5 presents the values of the unknown coefficients of Eq. (5). The accuracy of the equations is measured by the coefficient of determination, which is expressed by R^2. The values of R^2 shown in the tables indicate that the I_{ra} values predicted using the equations are sufficiently accurate. Equations (4) and (5) are valid for structures possessing a bi-linear material model without stiffness and strength degradations during earthquake. In addition, the mean values of I_{ra} predicted by Eq. (4) and the actual ones obtained from nonlinear time history analyses are compared in Fig. 16. Figure 17 shows the same comparison for Eq. (5).

$$I_{\mathrm{ra}}=\begin{cases}\left(\dfrac{a_1+a_2T+a_3R}{T^{a_4}}+R^{a_5}+a_6R\right)\dfrac{R-1}{R^{a_7}} & \text{Posotive polarity of aftershock}\\ \left(\dfrac{b_1+b_2T+b_3R}{T^{b_4}}+R^{b_5}+b_6R\right)\dfrac{R-1}{R^{b_7}} & \text{Negative polarity of aftershock}\end{cases} \tag{4}$$

$$\delta_{\max,\mathrm{m}}=c_1T+c_2R+c_3 \tag{5}$$

6 Numerical example

The residual displacement of the structure is obtained by the following steps.

- Determine an equivalent SDOF for the structure considered.
- Calculate T, R, α, δ_{y}, where δ_{y} is the yield

Table 3 Values of unknown coefficients of Eq. (4) for positive polarity of aftershock

Aftershock relative PGA	Post-yield stiffness ratio	a_1	a_2	a_3	a_4	a_5	a_6	a_7	R^2
γ=0.5	α=0	0.1256	-0.892	-0.018	1.2	0.1	0.6	2.0	0.93
	α=0.03	0.6277	0.006	-0.6241	0.15	0.87	-0.055	2.0	0.97
	α=0.05	-0.062	0.003	-0.538	0.1	0.07	0.5104	2.0	0.98
γ=0.8	α=0	0.087	-0.5626	-0.011	1.3	-0.35	0.7337	2.0	0.93
	α=0.03	0.065	0.035	-0.6236	0.11	0.37	0.5	2.0	0.98
	α=0.05	-0.002	1.115	-0.001	0.9	1.08	-1.277	1.5	0.98
γ=1.0	α=0	-2.727	5.178	3.574	0.5	3.87	-4.368	5.0	0.90
	α=0.03	-0.0837	0.0087	0.0118	0.3	-1.5	-0.0053	-0.05	0.97
	α=0.05	1.05	0.016	1.457	-0.03	1.0	-2.488	2.0	0.98
γ=1.2	α=0	-0.0022	0.054	-0.0005	2.8	-0.85	0.8159	2.0	0.90
	α=0.03	0.696	0.1273	-0.4171	0.28	0.85	-0.1317	2.25	0.97
	α=0.05	0.0555	0.068	-0.183	0.2	-0.12	0.1805	2.0	0.98
γ=1.5	α=0	0.7408	-0.2501	-0.088	0.7	-0.8	0.93	2.0	0.88
	α=0.03	0.3789	0.1219	-0.1914	0.4	-0.4	0.263	2.0	0.96
	α=0.05	0.964	0.1886	-0.4692	0.3	1.0	-0.3335	2.5	0.97

Table 4 Values of unknown coefficients of Eq. (4) for negative polarity of aftershock

Aftershock relative PGA	Post-yield stiffness ratio	b_1	b_2	b_3	b_4	b_5	b_6	b_7	R^2
γ=0.5	α=0	0.113	-0.7932	-0.017	1.2	0.3	0.497	2.0	0.93
	α=0.03	0.5755	0.003	-0.64	0.14	0.83	0.02	2.0	0.97
	α=0.05	-0.1693	0.007	-0.036	0.2	-0.5	0.03	1.2	0.97
γ=0.8	α=0	0.175	0.4	-0.023	0.75	1.0	-0.3623	2.0	0.9
	α=0.03	-0.048	0.084	0.006	0.62	-1.16	-0.013	0.7	0.98
	α=0.05	-0.1141	0.03	0.013	0.4	-1.0	-0.01	0.8	0.98
γ=1.0	α=0	0.09	0.1782	-0.009	0.8	-0.2	0.162	1.5	0.85
	α=0.03	-0.0177	0.2347	0.0007	0.8	-1.2	-0.0207	1.0	0.97
	α=0.05	-0.1055	0.07	-0.005	0.3	-0.5	-0.009	1.4	0.97
γ=1.2	α=0	0.1763	0.7367	-0.02	1.0	1.0	-0.3045	2.0	0.9
	α=0.03	0.7955	0.1	-0.4867	0.3	0.9	-0.035	2.4	0.97
	α=0.05	0.046	1.267	-0.016	0.9	1.08	-1.248	1.8	0.97
γ=1.5	α=0	1.365	0.098	-0.1593	0.45	-2.7	0.5665	1.8	0.87
	α=0.03	0.43	0.08	-0.2226	0.36	-0.4	0.2918	2.0	0.96
	α=0.05	0.2768	0.096	-0.1711	0.3	-0.6	0.2104	2.0	0.97

Table 5 Values of unknown coefficients of Eq. (5)

Post-yield stiffness ratio	c_1	c_2	c_3	R^2
α=0	0.09	0.023	-0.066	0.99
α=0.03	0.084	0.011	-0.04	0.99
α=0.05	0.083	0.009	-0.037	0.99

displacement.

- Obtain I_{ra} using Eq. (4) for both positive and negative polarities.
- Obtain $\delta_{max,m}$ using Eq. (5).
- Calculate $\delta_{res,a}$ by multiplying I_{ra} and $\delta_{max,m}$ for both polarities and the maximum one is considered as the response.

An equivalent SDOF system with these properties, T=2.2 s, R=4.0 and α=0.05 is considered. The bi-linear material model is assigned to this system and the yield displacement is considered to be 0.0029 m. This structure is analyzed under the Imperial Valley seismic sequence to obtain $\delta_{res,a}$ and this demand is computed as 0.039 and 0.04 for positive and negative polarities, respectively. On the other hand, I_{ra} is predicted by Eq. (4) for both polarities, with values of 0.2069 and 0.2077 for positive and negative polarities, respectively. After that, $\delta_{max,m}$= 0.1816 m is obtained using Eq. (5). Then $\delta_{res,a}$ is calculated using Eq. (1), namely $\delta_{res,a}$= $I_{ra}\times\ \delta_{max,m}$=0.2069×0.1816=0.0375 m for the positive polarity, and $\delta_{res,a}$= $I_{ra}\times\ \delta_{max,m}$=0.2077×0.1816=0.0377 m for the negative polarity. The final estimated value is the maximum of 0.0377 and 0.0375, namely 0.0377, which is very close to the actual one (0.039 or 0.04 for positive and negative polarities, respectively).

7 Summary and conclusions

The prediction of seismic demand of mainshock-damaged structures against aftershocks is a vital task which must be conducted using a rapid and robust method due to the uncertain occurrence time of subsequent seismic events. To this aim, this study

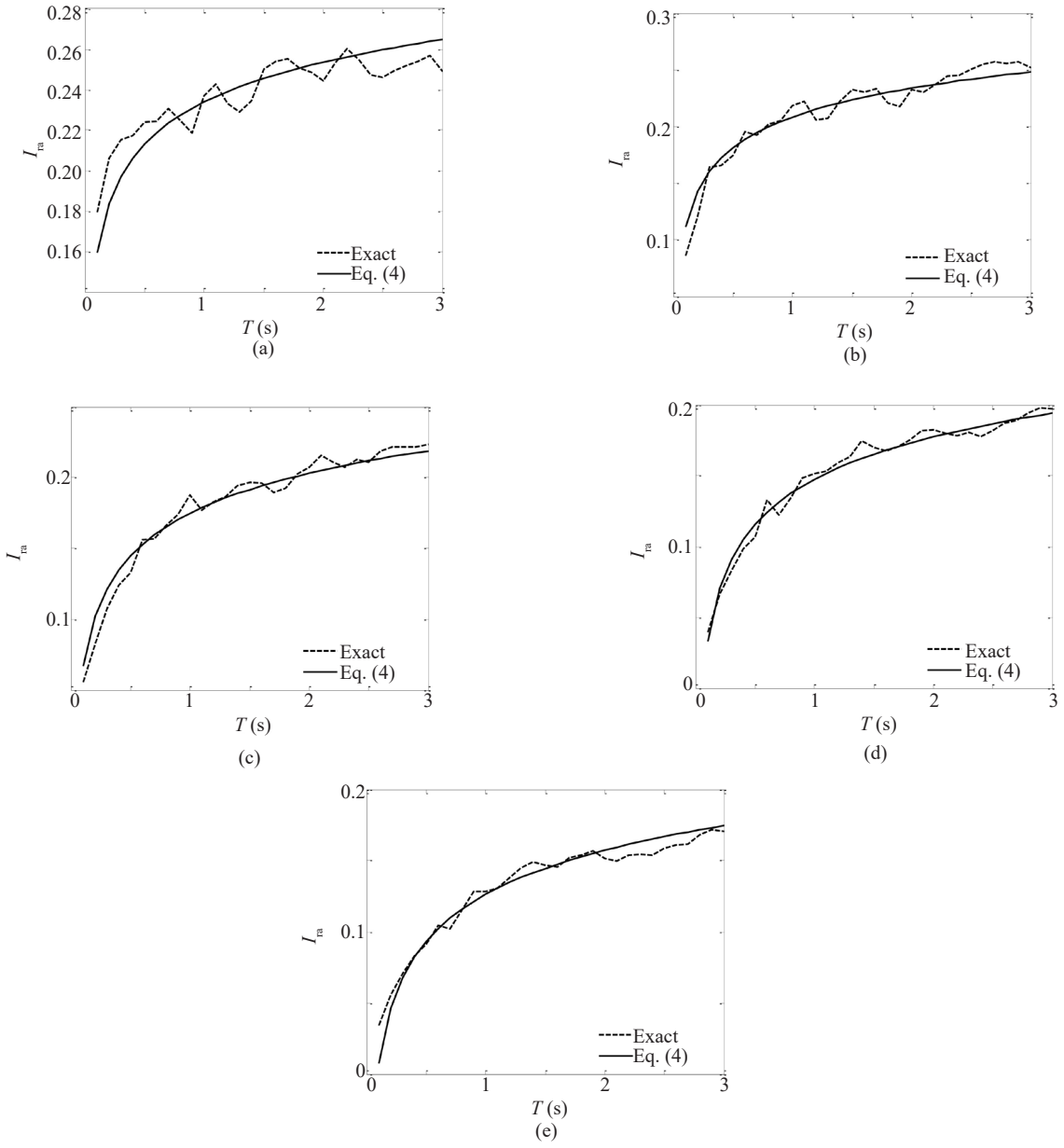

Fig. 16 Predicted values of I_{ra} against actual ones for: (a) R=2.0; (b) R=3.0; (c) R=4.0; (d) R=5.0; (e) R=6.0

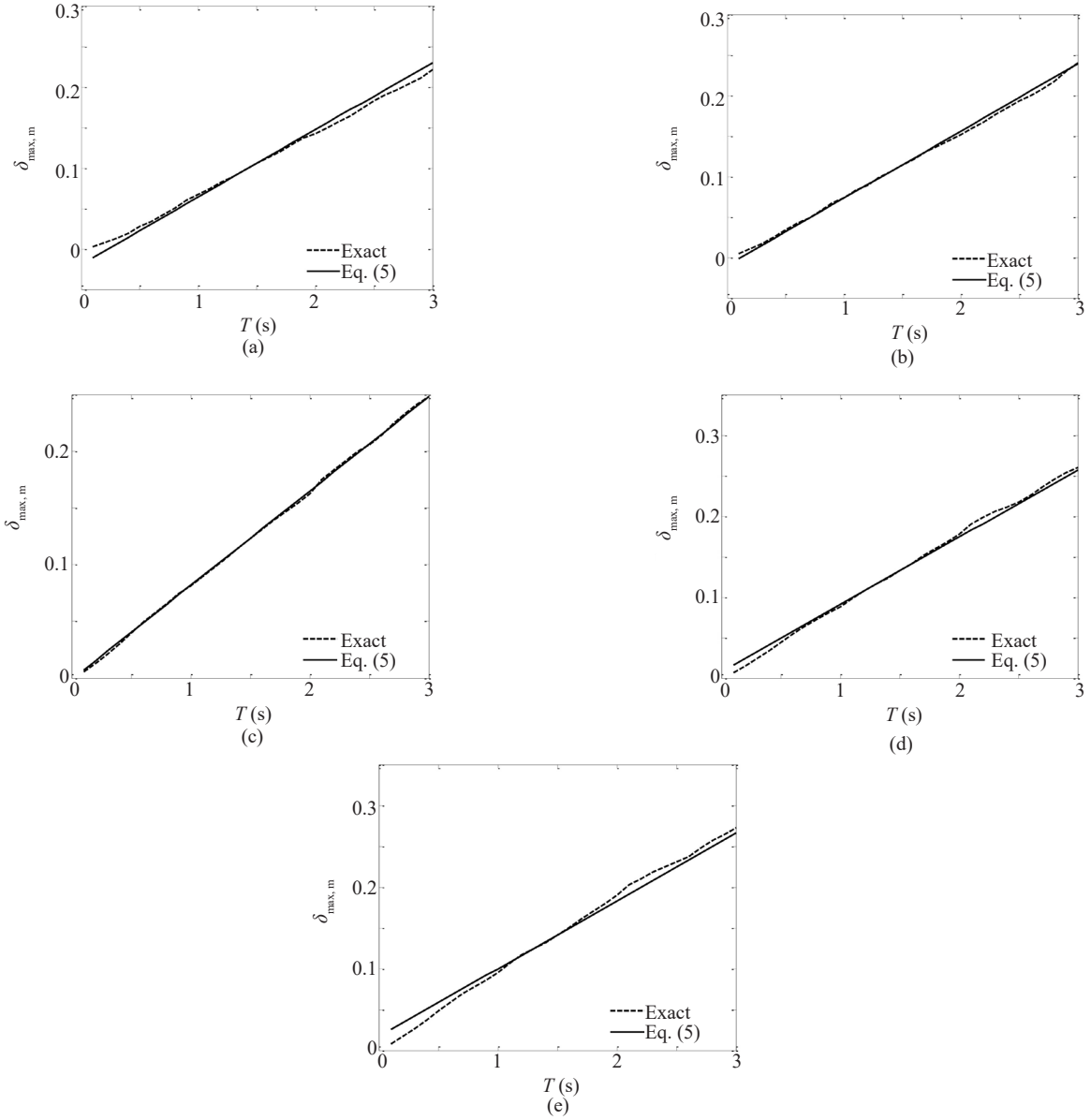

Fig. 17 Predicted values of $\delta_{max,m}$ against actual ones for: (a) R=2.0; (b) R=3.0; (c) R=4.0; (d) R=5.0; (e) R=6.0

introduces a simple and novel index to predict residual displacement of structures subjected to aftershocks. The index (shown by I_{ra}) is defined as a ratio between the residual displacement of mainshock-damaged structures against an aftershock and the peak inelastic displacement of intact ones subjected to a mainshock. A large set of real seismic sequences (330 sequences with five scale factors to maintain different aftershock relative intensities) are considered to develop constant strength-spectra based on the proposed index, considering a wide range of structural and seismic parameters. The most significant achievements of this study are:

- For the moderate-to-long period structural systems with linear elastic-perfectly plastic behavior (T>1.0 s, α=0), the larger values of I_{ra} are obtained from the moderate-moderate subset (moderate mainshock and moderate aftershock) compared to another magnitude-based subset (severe-moderate subset), approximately 43% and 37% for R=3.0 and R=5.0, respectively.
- The long-period structures (T>1.5 s) having lower values of the strength reduction factor (R≤3) built on site class C experience more values of I_{ra} (13% on average for three values of α) in comparison with those built in site class D.
- The structures with α=0 as well as T≥1.0 s are more vulnerable during near-field mainshocks, when they will be subjected to near-field aftershocks. In this regard, I_{ra} values estimated for these systems against a near-near subset are about 28% and 48% larger than the near-far and far-far subsets, respectively. This trend reduces as the post-yield stiffness ratio (α) increases.
- The short duration mainshocks and short duration aftershocks (SD-SD subset) cause higher I_{ra} for the flexible SDOF systems (T≥1.0 s) than LD-

SD and LD-LD subsets, by 28% and 65% on average, respectively. This proves that the seismic vulnerability of long structures after short duration mainshocks will be markedly affected during subsequent short duration aftershocks.

- The normalized residual displacement (I_{ra}) increases as the aftershock relative PGA (γ) increases. This increase is highlighted for systems with the linear elastic-perfectly plastic model, such that the values of I_{ra} predicted from γ=1.5 are wider (57% on average) than γ=0.5, in the case of R=3.0.
- I_{ra} tends to increase as the post-yield stiffness ratio (α) decreases; this pattern is more obvious when R increases. The I_{ra} values estimated for structures with R=6.0, and α=0 are larger than those systems possessing α=0.03 and α=0.05, by 232% and 369%, respectively. This proves that the use of high-strength elastic materials which leads to increased α, can be an efficient approach to decrease the residual displacement of structures.
- The normalized residual displacement increases as R increases, when α=0. This trend is inverse for α>0, i.e., α=0.03, and α=0.05. Namely, I_{ra} decreases as R increases, so that when R raises from 2.0 to 6.0, the decrease percentage of I_{ra} are approximately 66% and 98% for α=0.03 and α=0.05, respectively. As a result, the structures with α=0 and R=6.0 have the worst conditions from point of view of the structural safety after multiple earthquakes.
- Several analytical equations are presented to predict the proposed index for both cases of positive and negative polarities of aftershocks and the peak inelastic displacement which is necessary to calculate I_{ra}. The equations can be used for rapid seismic assessment of mainshock-damaged structures against subsequent aftershocks in terms of the residual displacement demand. These equations can be extended for a class of steel or RC buildings to estimate probable residual displacement/drift demands of these structures against aftershock.

References

Alessandri S, Giannini R and Paolacci F (2013), "Aftershock Risk Assessment and the Decision to Open Traffic on Bridges," *Earthquake Engineering & Structural Dynamics*, **42**(15): 2255–2275. https://doi.org/10.1002/eqe.2324

Amiri S and Bojórquez E (2019), "Residual Displacement Ratios of Structures Under Mainshock-Aftershock Sequences," *Soil Dynamics and Earthquake Engineering*, **121**: 179–193. https://doi.org/10.1016/j.soildyn.2019.03.021

Amiri S and Soroushian A (2017), "A Brief Review on Building Structural Analysis Regulations in Different Seismic Codes Research," *Bulletin of Seismology and Earthquake Engineering*, **20**: 1–24. (in Persian)

Ardakani SS, Saiidi MS and Somerville P (2021), "Residual Drift Spectra for RC Bridge Columns Subjected to Near-Fault Earthquakes," *Earthquake Engineering and Engineering Vibration*, **20**(1): 193–211. https://doi.org/10.1007/s11803-021-2014-y

ASCE/SEI 7-10 (2010), *Minimum Design Loads for Buildings and Other Structures*, American Society of Civil Engineers, Reston, VA, USA.

Atzori S, Tolomei C, Antonioli A, Merryman Boncori JP, Bannister S, Trasatti E, Pasquali P and Salvi S (2012), "The 2010–2011 Canterbury, New Zealand, Seismic Sequence: Multiple Source Analysis from InSAR Data and Modeling," *Journal of Geophysical Research: Solid Earth*, **117**. https://doi.org/10.1029/2012JB009178

Bojórquez E and Ruiz-García J (2013), "Residual Drift Demands in Moment-Resisting Steel Frames Subjected to Narrow-Band Earthquake Ground Motions," *Earthquake Engineering & Structural Dynamics*, **42**(11): 1583–1598. https://doi.org/10.1002/eqe.2288

Bommer JJ and MartÍnez-Pereira A (1999), "The Effective Duration of Earthquake Strong Motion," *Journal of Earthquake Engineering*, **3**: 127–172. https://doi.org/10.1080/13632469909350343

Bravo-Haro MA and Elghazouli AY (2018), "Permanent Seismic Drifts in Steel Moment Frames," *Journal of Constructional Steel Research*, **148**: 589–610. https://doi.org/10.1016/j.jcsr.2018.06.006

Burton HV and Sharma M (2017), "Quantifying the Reduction in Collapse Safety of Main Shock–Damaged Reinforced Concrete Frames with Infills," *Earthquake Spectra*, **33**(1): 25–44. https://doi.org/10.1193/121015eqs179m

Cai ZK, Zhou Z and Wang Z (2019), "Influencing Factors of Residual Drifts of Precast Segmental Bridge Columns with Energy Dissipation Bars," *Advances in Structural Engineering*, **22**(1): 126–140. https://doi.org/10.1177/1369433218780545

Cheng H, Li H, Wang D, Sun Z, Li G and Jin J (2016), "Research on the Influencing Factors for Residual Displacements of RC Bridge Columns Subjected to Earthquake Loading," *Bulletin of Earthquake Engineering*, **14**(8): 2229–2257. https://doi.org/10.1007/s10518-016-9902-y

Christopoulos C, Pampanin S and Nigel Priestley MJ (2003), "Performance-Based Seismic Response of Frame Structures Including Residual Deformations. Part I: Single-Degree of Freedom Systems," *Journal of Earthquake Engineering*, **7**(1): 97–118. https://doi.org/10.1080/13632460309350443

Dai K, Wang J, Li B and Hong HP (2017), "Use of Residual Drift for Post-Earthquake Damage Assessment of RC Buildings," *Engineering Structures*, **147**: 242–255.https://doi.org/10.1016/j.engstruct.2017.06.001

De Risi R, Sextos A, Zimmaro P, Simonelli A and Stewart JP (2018), "The 2016 Central Italy Earthquakes Sequence: Observations of Incremental Building

Damage," *Proceedings of the 11th U.S. National Conference on Earthquake Engineering, Los Angeles, California*.

Di Sarno L, Amiri S and Garakaninezhad A (2020), "Effects of Incident Angles of Earthquake Sequences on Seismic Demands of Structures," *Structures*, **28**: 1244-1251. https://doi.org/10.1016/j.istruc.2020.09.064

Di Sarno L and Amiri S (2019), "Period Elongation of Deteriorating Structures Under Mainshock-Aftershock Sequences," *Engineering Structures*, **196**, 109341. https://doi.org/10.1016/j.engstruct.2019.109341

Di Sarno L (2013), "Effects of Multiple Earthquakes on Inelastic Structural Response," *Engineering Structures*, **56**: 673–681. https://doi.org/10.1016/j.engstruct.2013.05.041

Di Trapani F and Malavisi M (2019), "Seismic Fragility Assessment of Infilled Frames Subject to Mainshock/Aftershock Sequences Using a Double Incremental Dynamic Analysis Approach," *Bulletin of Earthquake Engineering*, **17**(1): 211–235. https://doi.org/10.1007/s10518-018-0445-2

Doğangün A and Livaoğlu R (2006), "A Comparative Study of the Design Spectra Defined by Eurocode 8, UBC, IBC and Turkish Earthquake Code on R/C Sample Buildings," *Journal of Seismology*, **10**(3): 335–351. https://doi.org/10.1007/s10950-006-9020-4

Durante MG, Di Sarno L, Zimmaro P and Stewart JP (2018), "Damage to Roadway Infrastructure from 2016 Central Italy Earthquake Sequence," *Earthquake Spectra*, **34**(4): 1721–1737. https://doi.org/10.1193/101317eqs205m

Durucan C and Gümüş M (2018), "Direct Use of Peak Ground Motion Parameters for the Estimation of Inelastic Displacement Ratio of SDOF Systems Subjected to Repeated Far Fault Ground Motions," *Earthquake Engineering and Engineering Vibration*, **17**(4): 771–785. https://doi.org/10.1007/s11803-018-0475-4

Erochko J, Christopoulos C, Tremblay R and Choi H (2011), "Residual Drift Response of SMRFs and BRB Frames in Steel Buildings Designed According to ASCE 7-05," *Journal of Structural Engineering*, **137**(5): 589–599. https://doi.org/10.1061/(ASCE)ST.1943-541X.0000296

FEMA P58 (2012), *Seismic Performance Assessment of Buildings*, *Volume 1-Methodology*, Washington, DC: Federal Emergency Management Agency.

Franchin P and Pinto PE (2009), "Allowing Traffic over Mainshock-Damaged Bridges," *Journal of Earthquake Engineering*, **13**(5): 585–599. https://doi.org/10.1080/13632460802421326

Furtado A, Rodrigues H, Arêde A and Varum H (2017), "Assessment of the Mainshock-Aftershock Collapse Vulnerability of RC Structures Considering the Infills in-Plane and out-of-Plane Behaviour," *Procedia Engineering*, **199**: 619–624. https://doi.org/10.1016/j.proeng.2017.09.107

Furtado A, Rodrigues H, Varum H and Arêde A (2018), "Mainshock-Aftershock Damage Assessment of Infilled RC Structures," *Engineering Structures*, **175**: 645–660. https://doi.org/10.1016/j.engstruct.2018.08.063

Ghosh J, Padgett JE and Sánchez-Silva M (2015), "Seismic Damage Accumulation in Highway Bridges in Earthquake-Prone Regions," *Earthquake Spectra*, **31**(1): 115–135. https://doi.org/10.1193/120812eqs347m

Goda K, Pomonis A, Chian SC, Offord M, Saito K, Sammonds P, Fraser S, Raby A and Macabuag J (2013), "Ground Motion Characteristics and Shaking Damage of the 11th March 2011 M_w9.0 Great East Japan Earthquake," *Bulletin of Earthquake Engineering*, **11**(1): 141–170. https://doi.org/10.1007/s10518-012-9371-x

Goda K and Salami MR (2014), "Inelastic Seismic Demand Estimation of Wood-Frame Houses Subjected to Mainshock-Aftershock Sequences," *Bulletin of Earthquake Engineering*, **12**(2): 855–874. https://doi.org/10.1007/s10518-013-9534-4

Goda K and Taylor CA (2012), "Effects of Aftershocks on Peak Ductility Demand due to Strong Ground Motion Records from Shallow Crustal Earthquakes," *Earthquake Engineering & Structural Dynamics*, **41**(15): 2311–2330. https://doi.org/10.1002/eqe.2188

Guerrero H, Ruiz-García J and Ji T (2017), "Residual Displacement Demands of Conventional and Dual Oscillators Subjected to Earthquake Ground Motions Characteristic of the Soft Soils Of Mexico City," *Soil Dynamics and Earthquake Engineering*, **98**: 206–221. https://doi.org/10.1016/j.soildyn.2017.04.014

Guo JWW and Christopoulos C (2018), "A Probabilistic Framework for Estimating the Residual Drift of Idealized SDOF Systems of Non-Degrading Conventional and Damped Structures," *Earthquake Engineering & Structural Dynamics*, **47**(2): 479–496. https://doi.org/10.1002/eqe.2975

Harikrishnan MG and Gupta VK (2020), "Scaling of Residual Displacements in Terms of Elastic and Inelastic Spectral Displacements for Existing SDOF Systems," *Earthquake Engineering and Engineering Vibration*, **19**(1): 71–85. https://doi.org/10.1007/s11803-020-0548-z

Huff T (2016), "Estimating Residual Seismic Displacements for Bilinear Oscillators," *Practice Periodical on Structural Design and Construction*, **21**(2): 04016003. https://doi.org/10.1061/(ASCE)SC.1943-5576.0000282

Jalayer F and Ebrahimian H (2017), "Seismic Risk Assessment Considering Cumulative Damage Due to Aftershocks," *Earthquake Engineering & Structural Dynamics*, **46**(3): 369–389. https://doi.org/10.1002/eqe.2792

Ji D, Wen W, Zhai C and Katsanos EI (2018), "Residual Displacement Ratios of SDOF Systems Subjected to Ground Motions Recorded on Soft Soils," *Soil Dynamics and Earthquake Engineering*, **115**: 331–335. https://doi.

org/10.1016/j.soildyn.2018.09.001

Kunnath SK, Reinhorn AM and Lobo RF (1992), "IDARC Version 3.0: A Program for the Inelastic Damage Analysis of Reinforced Concrete Structures," *Technical Report No. NCEER- 92–0022*, National Center for Earthquake Engineering Research, State University of New York at Buffalo, USA.

Lee WK and Billington SL (2011), "Performance-Based Earthquake Engineering Assessment of a Self-Centering, Post-Tensioned Concrete Bridge System," *Earthquake Engineering & Structural Dynamics*, **40**(8): 887–902.

Li Q and Ellingwood BR (2007), "Performance Evaluation and Damage Assessment of Steel Frame Buildings Under Main Shock–Aftershock Earthquake Sequences," *Earthquake Engineering & Structural Dynamics*, **36**(3): 405–427. https://doi.org/10.1002/eqe.667

Li Y, Song R and Van de Lindt J (2014), "Collapse Fragility of Steel Structures Subjected to Earthquake Mainshock-Aftershock Sequences," *Journal of Structural Engineering*, **140**(12): 04014095. https://doi.org/10.1061/(ASCE)ST.1943-541X.0001019

Liossatou E and Fardis MN (2015), "Residual Displacements of RC Structures as SDOF Systems," *Earthquake Engineering & Structural Dynamics*, **44**(5): 713–734. https://doi.org/10.1002/eqe.2483

Liossatou E and Fardis MN (2016), "Near-Fault Effects on Residual Displacements of RC Structures," *Earthquake Engineering & Structural Dynamics*, **45**(9): 1391–1409. https://doi.org/10.1002/eqe.2712

López-Barraza A, Bojórquez E, Ruiz SE and Reyes-Salazar A (2013), "Reduction of Maximum and Residual Drifts on Posttensioned Steel Frames with Semirigid Connections," *Advances in Materials Science and Engineering*, 2013, 11. https://doi.org/10.1155/2013/192484

Mazzoni S, Castori G, Galasso C, Calvi P, Dreyer R, Fischer E, Fulco A, Sorrentino L, Wilson J, Penna A and Magenes G (2018), "2016–2017 Central Italy Earthquake Sequence: Seismic Retrofit Policy and Effectiveness," *Earthquake Spectra*, **34**(4): 1671–1691. https://doi.org/10.1193/100717eqs197m

Mazzoni S, McKenna F, Scott MH and Fenves GL (2006), *OpenSees Command Language Manual*, Pacific Earthquake Engineering Research (PEER) Center, 264.

Nazari N, Van de Lindt JW and Li Y (2015), "Effect of Mainshock-Aftershock Sequences on Woodframe Building Damage Fragilities," *Journal of Performance of Constructed Facilities*, **29**(1): 04014036. https://doi.org/10.1061/(ASCE)CF.1943-5509.0000512

Omranian E, Abdelnaby AE and Abdollahzadeh G (2018), "Seismic Vulnerability Assessment of RC Skew Bridges Subjected to Mainshock-Aftershock Sequences," *Soil Dynamics and Earthquake Engineering*, **114**: 186–197. https://doi.org/10.1016/j.soildyn.2018.07.007

Oyarzo-Vera C and Chouw N (2008), "Comparison of Record Scaling Methods Proposed by Standards Currently Applied in Different Countries," *Proceedings of the 14th World Conference on Earthquake Engineering* (*14 WCEE*), Beijing, China.

Papaloizou L, Polycarpou P, Komodromos P, Hatzigeorgiou GD and Beskos DE (2016), "Two-Dimensional Numerical Investigation of the Effects of Multiple Sequential Earthquake Excitations on Ancient Multi-Drum Columns," *Earthquakes and Structures*, **10**(3): 495–521. https://doi.org/10.12989/eas.2016.10.3.495

PEER Ground Motion Database, Pacific Earthquake Engineering Research Center. (https://ngawest2.berkeley.edu/)

Pu W and Wu M (2018), "Ductility Demands and Residual Displacements of Pinching Hysteretic Timber Structures Subjected to Seismic Sequences," *Soil Dynamics and Earthquake Engineering*, **114**: 392–403. https://doi.org/10.1016/j.soildyn.2018.07.037

Qiang HL, Feng P and Qu Z (2019), "Seismic Responses of Postyield Hardening Single–Degree-of-Freedom Systems Incorporating High-Strength Elastic Material," *Earthquake Engineering & Structural Dynamics*, **48**(6): 611–633. https://doi.org/10.1002/eqe.3151

Raghunandan M, Liel AB, Ryu H, Luco N and SR U (2012), "Aftershock Fragility Curves and Tagging Assessments for a Mainshock-Damaged Building," *Proceedings of the 15th World Conference on Earthquake Engineering* (*15 WCEE*), Lisbon, Portugal.

Raghunandan M, Liel AB and Luco N (2015), "Aftershock Collapse Vulnerability Assessment of Reinforced Concrete Frame Structures," *Earthquake Engineering & Structural Dynamics*, **44**(3): 419–439. https://doi.org/10.1002/eqe.2478

Ramirez CM and Miranda E (2012), "Significance of Residual Drifts in Building Earthquake Loss Estimation," *Earthquake Engineering & Structural Dynamics*, **41**(11): 1477–1493. https://doi.org/10.1002/eqe.2217

Rosenblueth E and Meli R (1986), "The 1985 Mexico Earthquake," *Concrete International*, **8**(5): 23–34.

Ruiz-García J and Aguilar JD (2015), "Aftershock Seismic Assessment Taking into Account Postmainshock Residual Drifts," *Earthquake Engineering & Structural Dynamics*, **44**(9): 1391–1407. https://doi.org/10.1002/eqe.2523

Ruiz-García J and Chora C (2015), "Evaluation of Approximate Methods to Estimate Residual Drift Demands in Steel Framed Buildings," *Earthquake Engineering & Structural Dynamics*, **44**(15): 2837–2854. https://doi.org/10.1002/eqe.2611

Ruiz-García J and Guerrero H (2017), "Estimation of Residual Displacement Ratios for Simple Structures Built on Soft-Soil Sites," *Soil Dynamics and Earthquake*

Engineering, **100**: 555–558. https://doi.org/10.1016/j.soildyn.2017.07.008

Ruiz-García J, Marín MV and Terán-Gilmore A (2014), "Effect of Seismic Sequences in Reinforced Concrete Frame Buildings Located in Soft-Soil Sites," *Soil Dynamics and Earthquake Engineering*, **63**: 56–68. https://doi.org/10.1016/j.soildyn.2014.03.008

Ruiz-García J and Miranda E (2006), "Residual Displacement Ratios for Assessment of Existing Structures," *Earthquake Engineering & Structural Dynamics*, **35**(3): 315–336. https://doi.org/10.1002/eqe.523

Ruiz-García J and Negrete-Manriquez JC (2011), "Evaluation of Drift Demands in Existing Steel Frames Under As-Recorded Far-Field and Near-Fault Mainshock–Aftershock Seismic Sequences," *Engineering Structures*, **33**(2): 621–634. https://doi.org/10.1016/j.engstruct.2010.11.021

Ruiz-García J, Terán-Gilmore A and Díaz G (2012), "Response of Essential Facilities Under Narrow-Band Mainshock–Aftershock Seismic Sequences," *Proceedings of the 15th World Conference on Earthquake Engineering* (*15 WCEE*), Lisbon, Portugal.

Ruiz-García J, Yaghmaei-Sabegh S and Bojórquez E (2018), "Three-Dimensional Response of Steel Moment-Resisting Buildings under Seismic Sequences," *Engineering Structures*, **175**: 399–414. https://doi.org/10.1016/j.engstruct.2018.08.050

Salami MR and Goda K (2013), "Seismic Loss Estimation of Residential Wood-Frame Buildings in Southwestern British Columbia Considering Mainshock-Aftershock Sequences," *Journal of Performance of Constructed Facilities*, **28**(6): A4014002.

Santarsiero G, Di Sarno L, Giovinazzi S, Masi A, Cosenza E and Biondi S (2018), "Performance of the Healthcare Facilities During the 2016–2017 Central Italy Seismic Sequence," *Bulletin of Earthquake Engineering*, **17**(10): 5701–5727. https://doi.org/10.1007/s10518-018-0330-z

Shokrabadi M and Burton HV (2018), "Risk-Based Assessment of Aftershock and Mainshock-Aftershock Seismic Performance of Reinforced Concrete Frames," *Structural Safety*, **73**: 64–74. https://doi.org/10.1016/j.strusafe.2018.03.003

Shu Z and Zhang J (2018), "Dimensional Estimation of Residual-Drift Demands for Bilinear Bridges Under Near-Fault Ground Motions," *Journal of Bridge Engineering*, **23**(11), 04018087. https://doi.org/10.1061/(ASCE)BE.1943-5592.0001298

Singh DK, Mandal A, Karumanchi SR, Murmu A and Sivakumar N (2018), "Seismic Behaviour of Damaged Tunnel During Aftershock," *Engineering Failure Analysis*, **93**: 44–54. https://doi.org/10.1016/j.engfailanal.2018.06.028

Tesfamariam S and Goda K (2015), "Seismic Performance Evaluation Framework Considering Maximum and Residual Inter-Story Drift Ratios: Application to Non-Code Conforming Reinforced Concrete Buildings in Victoria, BC, Canada," *Frontiers in Built Environment* 1, 18. https://doi.org/10.3389/fbuil.2015.00018

Tesfamariam S and Goda K (2017), "Impact of Earthquake Types and Aftershocks on Loss Assessment of Non-Code-Conforming Buildings: Case Study with Victoria, British Columbia," *Earthquake Spectra*, **33**(2): 551–579. https://doi.org/10.1193/011416eqs013m

Tesfamariam S, Goda K and Mondal G (2015), "Seismic Vulnerability of Reinforced Concrete Frame with Unreinforced Masonry Infill Due to Main Shock–Aftershock Earthquake Sequences," *Earthquake Spectra*, **31**(3): 1427–1449. https://doi.org/10.1193/042313eqs111m

Tolentino D, Flores RB and Alamilla JL (2018), "Probabilistic Assessment of Structures Considering the Effect of Cumulative Damage Under Seismic Sequences," *Bulletin of Earthquake Engineering*, **16**(5): 2119–2132. https://doi.org/10.1007/s10518-017-0276-6

Trifunac D and Brady A (1975), "A Study on the Duration of Strong Earthquake Ground Motion," *Bulletin of the Seismological Society of America*, **65**(3): 581–626.

Wang G, Wang Y, Lu W, Yan P and Chen M (2018), "Earthquake Direction Effects on Seismic Performance of Concrete Gravity Dams to Mainshock-Aftershock Sequences," *Journal of Earthquake Engineering*, 1–22. https://doi.org/10.1080/13632469.2018.1453423

Wang G, Wang Y, Lu W, Yan P, Zhou W and Chen M (2017), "Damage Demand Assessment of Mainshock-Damaged Concrete Gravity Dams Subjected to Aftershocks," *Soil Dynamics and Earthquake Engineering*, **98**: 141–154. https://doi.org/10.1016/j.soildyn.2017.03.034

Wen W, Ji D and Zhai C (2020), "Ground Motion Rotation for Mainshock-Aftershock Sequences: Necessary or not?" *Soil Dynamics and Earthquake Engineering*, **130**, 105976. https://doi.org/10.1016/j.soildyn.2019.105976

Wen W, Zhai C and Ji D (2018), "Damage Spectra of Global Crustal Seismic Sequences Considering Scaling Issues of Aftershock Ground Motions," *Earthquake Engineering & Structural Dynamics*, **47**(10): 2076–2093. https://doi.org/10.1002/eqe.3056

Wen W, Ji D, Zhai C, Li X and Sun P (2018), "Damage spectra of the Mainshock-Aftershock Ground Motions at Soft Soil Sites," *Soil Dynamics and Earthquake Engineering*, **115**: 815–825. https://doi.org/10.1016/j.soildyn.2018.08.016

Wen W, Zhai C, Ji D, Li S and Xie L (2017), "Framework for the Vulnerability Assessment of Structure Under Mainshock-Aftershock Sequences," *Soil Dynamics and Earthquake Engineering*, **101**: 41–52. https://doi.org/10.1016/j.soildyn.2017.07.002

Yu XH, Li S, Lu DG and Tao J (2018), "Collapse Capacity of Inelastic Single-Degree-of-Freedom

Systems Subjected to Mainshock-Aftershock Earthquake Sequences," *Journal of Earthquake Engineering*: 1–24. https://doi.org/10.1080/13632469.2018.1453417

Zhai C, Ji D, Wen W, Li C, Lei W and Xie L (2018), "Hysteretic Energy Prediction Method for Mainshock-Aftershock Sequences," *Earthquake Engineering and Engineering Vibration*, **17**(2): 277–291. https://doi.org/10.1007/s11803-018-0441-1

Zhai CH, Wen WP, Li S and Xie LL (2015), "The Ductility-Based Strength Reduction Factor for the Mainshock–Aftershock Sequence-Type Ground Motions," *Bulletin of Earthquake Engineering*, **13**(10): 2893–2914. https://doi.org/10.1007/s10518-015-9744-z

Zhang S, Wang G and Sa W (2013), "Damage Evaluation of Concrete Gravity Dams Under Mainshock–Aftershock Seismic Sequences," *Soil Dynamics and Earthquake Engineering*, **50**: 16–27. https://doi.org//10.1016/j.soildyn.2013.02.021